Saturation Spectroscopy using a 404.7 nm for Probing Level Populations at TRINAT

Shawn Fostner
University of Guelph

Supervisor: John Behr

August 29, 2002

Abstract

In order to perform high precision, polarization measurements using TRIUMF's Neutral-Atom-Trap (TRINAT) it is important to know the polarization to better than 0.1% . This is can currently be checked to 1% using model dependent probes. Another approach under consideration uses a 404.7 nm diode laser locked to the $4^2S_{1/2}$ to $5^2P_{1/2}$ ^{39}K transition. The laser will then be frequency shifted using a 300 Mhz double pass AOM and used to probe the Zeeman split levels of the atoms in the trap. In order to do so, it is necessary to have the laser frequency locked to accuracy on the order of the 1MHz Zeeman splittings. Preliminary indications are that this is possible though as of the time of writing had not been achieved. In the process of locking this laser, an estimate of the residual isotope shift is measured and presented.

Contents

List of Figures

1 Introduction

The Triumf Neutral Atom Trap (TRINAT) group is attempting to trap and polarize Potassium atoms to study nuclear beta decay. In order to polarize and observe the atoms they must first be carefully confined to a small region in a relatively stable and flexible trap. To do this TRINAT uses a Magneto-Optical Trap or MOT (also known as a Zeeman optical trap) to trap neutral atoms. A MOT is formed by applying a weak quadrupole magnetic field centered on the trap region, with 6 counter propagating circularly polarized beams which are tuned just below the atomic resonance. Each of the 2 beams in a given dimension are oppositely cirularly polarized. The detuning causes the atoms to slow and cool, as they are Doppler shifted closer to resonance when moving into the beam of light. The confinement comes about because of the Zeeman splitting of the atoms' atomic levels due to the magnetic field. This results in a different absorption of the σ^+ and σ^- light which then causes a scattering force towards the center of the trap. [1] The MOT used at TRINAT actually involves a MOT where the atoms are first stopped, and a second MOT where the beta decays can be observed in a low background environment.

In most of the experiments currently planned for TRINAT the atoms in the trap must be polarized. In a typical MOT the polarization is ~ 0. For TRINAT to achieve polarization the MOT is turned off and the atoms are optically pumped via a 770 nm laser locked to the $4^2S_{1/2}$ - $4^2P_{1/2}$ state of ^{39}K [2]. This laser will then be frequency shifted using an Acousto-Optic-Modulator or AOM to the pumping frequencies desired. To probe the level populations achieved using the "red" laser a similar "blue" diode laser at 404.7 nm was purchased. The vacuum wavelength of the transition is actually 24701.38 cm^{-1} or 404.83 nm [3], however the laser frequency is quoted in air. To achieve the necessary laser width requires locking the laser to an external cell. The locking method and related calculations are described below. This is possible using this laser because the $4^2S_{1/2}$ - $5^2P_{1/2}$ transition has a natural linewidth of 1.1 Mhz compared to the 6 Mhz linewidth of the $4^2P_{1/2}$ transition.

1.1 Saturation Spectroscopy

In order to use the laser it needs to be locked precisely to a known atomic transition. A glass cell filled with potassium vapour containing approximately 93% ^{39}K and 7% ^{41}K is used. Saturation spectroscopy is a standard technique for obtaining doppler free absorption spectra which can then be locked to. The laser is scanned over a small frequency range containing one or more atomic resonances. The velocity component of the atoms parallel to the laser propagation direction doppler shifts the laser frequency in the frame of reference of the atoms. Those atoms in which the doppler shifted frequency falls within the linewidth of a transition can then interact with the laser. This gives rise to broad absorption profiles which are several Ghz wide for the transitions accessible to this laser. In order to eliminate the doppler broadened width of the signal, saturation spectroscopy requires two counter-propagating beams from the same laser overlapping in the potassium cell. In our case it is assumed that one of the beams has a much higher power than the other, the higher power beam being the pump beam and the lower being the probe beam. As the beams propagate in different directions in the cell, the doppler shift of the laser light from each beam with respect to a given velocity class of atoms is opposite. Thus, for any frequency not equal to the transition frequency only the velocity class $v_Z = +(\omega - \omega_0 \mp \gamma_s/2)/k$ with w and w_0 the laser frequency and transition frequency respectively, γ_s the broadened width, and k= k_z the laser wave number in the propagation direction will effectively be on resonance. On resonance however only atoms moving perpendicular to the beam, with velocity $v_z = (0 \mp \gamma_s/2)/k \approx 0$ in the parallel direction are capable of interacting with the laser. As a result of the negligible doppler shift for these atoms they can interact with both beams. This means that it is possible for the pump beam to saturate the transition and cause a dip in the absorption profile of the other beam which can be detected. This dip, known as the Lamb dip [4], is centered about the transition frequency, and has a linewidth that can approach that of the natural linewidth of the transition.

The saturation peaks observed using this technique correspond to the hyperfine structure of the levels themselves. This will be discussed further in the following section. What is important to note, is that for a three level system, with a ground and two excited states, one would expect to see only two saturation peaks. What is in fact observed is three peaks! This is simple to understand if we consider a situation where the laser frequency is half-way between two states. What then occurs is that the doppler shifts for the light with respect to a particular velocity group are equal and opposite and so for one particular velocity class both the upper and lower of the excited states can be excited. The pump beam depletes the ground state population by exciting one of the transitions. This leads to a drop in the absorption for the probe beam, resulting in a peak half-way between the two resonances. In situations where there is a common upper level for a transition and split ground state the effect is similar, though the reasoning slightly different. In this case the pump beam increases the population in the common upper state and from this state spontaneous emission occurs to both ground states. This actually increases the absorption of the probe beam. In normal absorption the K atoms would be quickly hyperfine pumped into the other ground state, no longer aborbing light. As the beam is between both resonances the atoms are pumped back, and can thereby absorb more.

In a complicated system the number of saturation peaks, cross over peaks, and crossover dips can form a large number of peaks and understanding where the lock on the laser rests can be difficult. This will be looked at with respect to the potassium resonances shortly.

2 Hyperfine structure

The peaks observed using saturation spectroscopy are separated by the hyperfine structure of the ground and first excited state of ^{39}K. The hyperfine splitting is a result of the interaction of the magnetic dipole of the nucleus with the magnetic field of the atomic electrons and the electric quadrupole moment of the nucleus with the atomic electrons. It can be shown that these levels have good angular momentum $\vec{F} = \vec{I} + \vec{J}$ where I is the total nuclear angular momentum and J the total atomic angular momentum. [5] This then gives rise to a shift in frequency of each level given by the well known formula

$$\Delta\nu = \frac{AK}{2} + \frac{B}{4}\frac{\frac{3}{2}K(K+1) - 2I(I+1)J(J+1)}{I(2I-1)J(2J-1)}$$

where A and B are factors specific to each level and $K = F(F+1) - I(I+1) - J(J+1)$. [6].

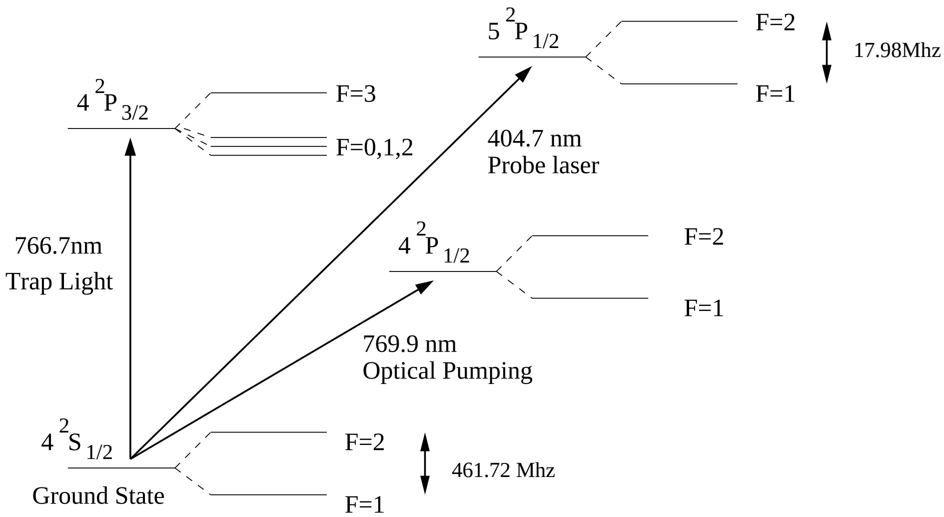

Figure 1: The ground state of potassium along with the excited states of interest. The level splittings shown are not to scale.

If A and B have been measured, it becomes a relatively simple matter to calculate the hyperfine splittings of both the ground state and $5^2P_{1/2}$ excited state for ^{39}K. The splitting for the 4p states is also known, [7] and is relevant for the trap laser and optical pumping, but not for this laser. For the excited state we have two levels with quantum numbers $I = 3/2$, $J = 1/2$, and F=1 and F=2 respectively. The electric quadrupole contribution is exactly zero for $J = 1/2$. Arimondo et al. [6] lists two experimental results for A with the most precise being 8.99(15) Mhz. Using this we arrive at a splitting of +6.74(11) Mhz for the F=2 state and -11.24(19) Mhz for the F=1 state. Thus the splitting is 17.98(22) Mhz for this state in ^{39}K.This is considerably smaller than that of the ground state and is apparent in the spectra obtained.

The ground state splitting has however been extremely well measured and of the values given by Arimondo [6] the most precise is 461.7197201(6) Mhz. For the purposes of this work, in which the laser frequency is known only to 1 Mhz, this level of precision is not required. While the A factor and hence the specific splitting of the ground states are not given, they can be easily worked out by going backwards from the splitting. Again in this case there is no quadrupole contribution, so we need only solve for A which is

230.859 Mhz. We will take this as exact given the high level of precision in the splitting compared to that required here. This tells us the F=2 state is moved up 173.14 Mhz and the F=1 state is moved down by 288.57 Mhz.

The hyperfine splitting for ^{41}K differs only in the A factor, as the nuclear spin and angular momentum numbers are identical. The ground state splitting for ^{41}K has been measured to be 254.014 Mhz [6]. In a similar manner to the ^{39}K ground state calculation we find $A = 127.01Mhz$ and F=2 moves up 95.26 Mhz whereas F=1 moves down by 158.76 Mhz.

The $5^2P_{1/2}$ excited state in which we are interested is not given, and to the best of our knowledge has not been measured for ^{41}K. The splitting can however be estimated to a reasonable degree of accuracy by noting that the A factor is given as $A = \frac{\mu_N g_I B_{el}}{J}$ and so should scale with the nuclear moments as

$$\begin{aligned} \frac{A}{A'} &= \frac{\mu I'}{\mu' I} \\ &or \quad \frac{g_I}{g_I'} \end{aligned}$$

assuming the magnetisation is point-like and thus ignoring possible hyperfine anomalies [5]. If we note that spins of ^{39}K and ^{41}K are the same then we need only the nuclear magnetic moment. For ^{39}K and ^{41}K the moments are 0.39150731(12) and 0.21489274(12) respectively, in units of the nuclear magneton [8]. From the measured A in ^{39}K the A factor for the ^{41}K $5^2P_{1/2}$ is then 4.93(8) Mhz. Thus the splittings are +3.70(6) and -6.2(1) Mhz for the F=2 and F=1 state respectively. The spectroscopic lines expected are shown in Fig 2. It should be noted that the changes in frequency calculated using the hyperfine formula are in absolute energies, thus the changes in frequency in the spectroscopic signals will move in opposite directions for the ground state. Thus the F=1 ground state has a lower energy and thus a higher transition frequency whereas this is reversed for the excited state splittings.

2.1 The Isotope Shift

What we have calculated here are the splittings for both potassium isotopes. Taking these into account we know where to expect the saturation spectroscopy peaks for each group independently. In order to know what the separation between the two isotopes is, we would need to know the isotope

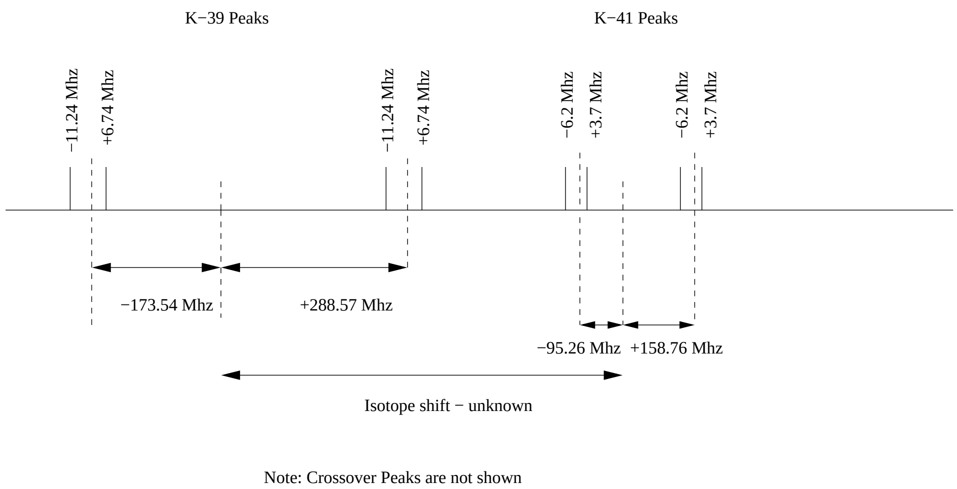

Figure 2: Schematic of the expected transition frequencies

shift. This is unfortunately difficult to calculate. There are several components to the isotope shift: the mass shift, field shift, and specific mass shift. These three components sum to give the isotope shift

$$IS = NMS + SMS + FS$$

The mass shift or normal mass shift can be simply thought of as the result of having a nucleus of finite mass. Classically the nucleus and an electron can be thought of in a reduced mass scheme. This means that without an infinite nuclear mass the mass of different isotopes will affect the atomic levels [9]. If H represents the heavy isotope and L the light isotope then the normal mass shift is exactly given by

$$\frac{\nu_H - \nu_L}{\nu_L} = \frac{m(M_H - M_L)}{M_L(M_H + m)}$$

$$or$$

$$\Delta\nu = \frac{m(A_H - A_L)}{UA_H A_L}\nu_L$$

[10] where M refers to the nuclear mass, m the electron mass, A the mass in atomic mass units, and U the atomic mass unit. The field shift is the change in the energy levels of the electrons as the nuclear charge density

changes with additional neutrons. This change in charge density affects only those atomic electrons which have a non zero probability of being found in the nucleus itself. Outside this region the nuclear charge clearly remains the same and thus the field is independent of the neutron number. The field shift is approximately given by

$$\begin{aligned}\Delta\nu &= F\delta < r^2 > \\ F &= \frac{\pi {a_0}^3}{Z} f(z)\Delta|\psi(0)|^2\end{aligned}$$

where r is the nuclear radius, $\psi(0)$ the electronic wavefunction at the nucleus, f(z) a relativistic factor to be calculated, and a_0 the Bohr radius [10].

The specific mass shift is much more difficult to calculate. It comes about because of correlations between the orbiting electrons. Recent advances have been made in theoretically calculating the SMS using many body perturbation theory but that will not be done here [11]. The shift can be represented as

$$SMS = S\frac{A_H - A_L}{A_H A_L}$$

[10]

The parameter S masks the difficult calculations to calculate the SMS. In practice it is desirable to know the SMS in order to separate out the FS from the isotope shift and then get information about the charge radius of the nucleus.

In this work we are interested in the isotope shift of the $4^2S_{1/2}$ to $5^2P_{1/2}$ transitions for ^{39}K and ^{41}K potassium. Using the standard atomic masses for these two isotopes and knowing the vacuum frequency of the transition to be 24701.38 cm^{-1} or 404.83 nm the NMS is found to be 508.6 Mhz. This is by far the dominant component of the shift. The SMS itself for this level is not known, or rather has not been calculated though we will make an estimate of it in 4.5. We can get an idea of the order of magnitude from the known SMS in the $4^2S_{1/2}$ to $4^2P_{1/2}$ transition. Here it is found to be -19.92 Mhz. The FS is -12.91 Mhz for this transition [12]. Using the same FS for our estimate is reasonable under these circumstances if we refer to Wendt 84 [13] who shows that the difference in $6p_{1/2}$ and $6p_{3/2}$ states in Ba +1 is on the order of 2.5 % . The $6p_{1/2}$ state has nuclear overlap only as a result of relativistic corrections. We expect here that the states in K to have smaller overlap. So as an approximation it is reasonable to use -12.91Mhz for the field shift. This gives us a total of 475.77 Mhz. The uncertainty in this is difficult to estimate as the SMS is essentially unknown. We can compare this to experiment shortly however.

3 Beam Characteristics and Alignment

The focus of this report is not the alignment of the beam and procedures to optimize its quality. That in mind, it is important to note a few things. Refer to Fig 3 for general setup of the laser optics installed this summer. The beam coming directly from the diode laser has good polarization and is slightly distorted spatially. As a result, in the first leg of the beam path an anamorphic prism pair was inserted as well a telescope. The prism pair changes the elliptical beam to give a good circular cross-section and the telescope reduces the size and forces the beam to be largely parallel, with a diameter of around 1 mm. At this point in the path a set of two optical isolators are set up to reduce feedback into the laser cavity. Following this the beam has approximately 1.4 mW peak power with vertical polarization. Using a quarter wave plate and polarizing beamsplitting cube the beam is then split into two roughly equal beams which are sent to the saturation spectroscopy setup and the other to the AOM and trap. It is important to note that despite the telescope which was carefully tuned to make the beam parallel, over a path approaching a meter around the table the beam quality suffers significantly, beginning to diverge and become distorted. As a result it was found that the AOM could not be placed further downstream since the AOM requires a good beam quality to function properly. Also, a number of unforeseen difficulties particular to this wavelength were also observed. The most obvious of these is that the majority of optics is optimized for IR wavelengths. It is possible to find laser optics at these wavelengths but more difficult and expensive. In order to do these tests and assess the feasibility of using this AOM a version without 405 nm coatings is used currently. This leads to significant reflection losses. Leaving this aside we will look more at the frequency of the laser and the locking setup.

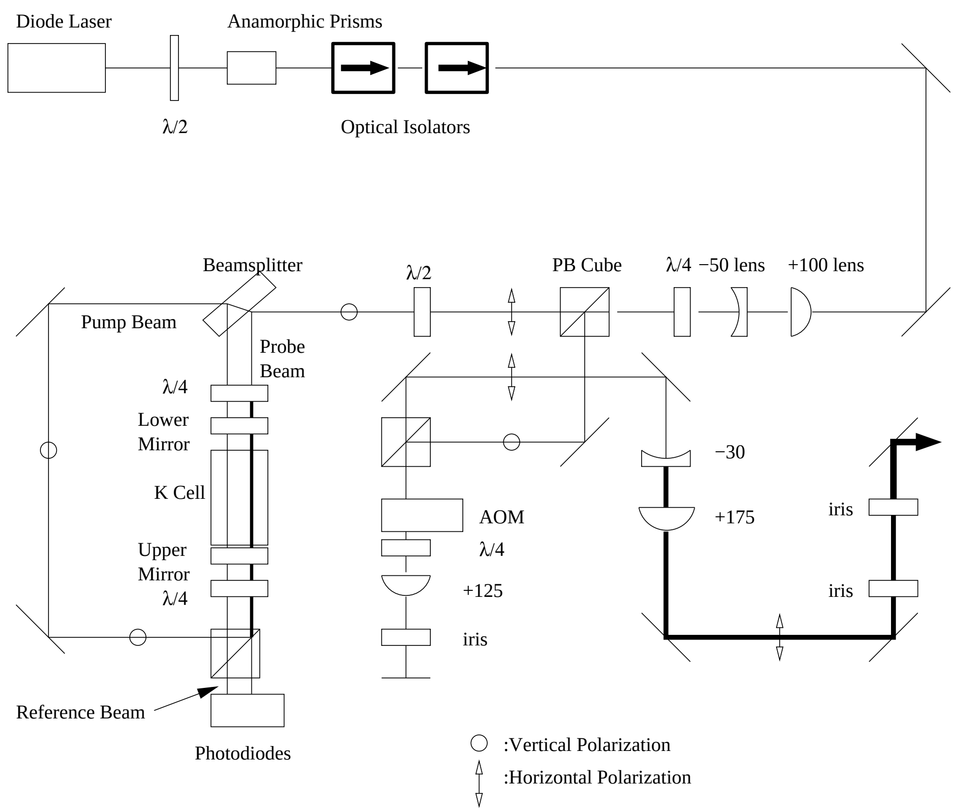

Figure 3: The 404.7 nm laser table

4 Locking the Laser with Saturation Spectroscopy

4.1 Frequency Tuning

The frequency of a diode laser is set crudely by adjustment of the internal grating. Once this is set to the frequency region of interest the laser frequency can be adjusted via a voltage controlled piezo electric transducer or PZT. Shipped with this laser are a precise current control supply and scan control box capable of sending a 0-150 V offset to the laser PZT and adding a further scan ramp of up to 60 V. The laser when shipped was set to 404.8 nm air wavelength. In order to get to the frequency at which the relevant lines lie it was necessary to either apply a large offset to the piezo actuator or physically tune the grating of the laser. For the majority of the setup and tests with the laser this summer the offset option was used, running the scan control around 140 V. To find the crude region of interest the laser was set up with the probe and pump beams running through the cell. Using an IR viewer one could detect the secondary flourescence as atoms in the cell were excited to the $5^2P_{1/2}$ state and would decay to the ground state through multiple processes, including the lower $4^2P_{1/2}$ levels. By tuning the current and voltage the frequency could be crudely set such that the resonance was observed. For future use a security camera and tv have been set up, which allows a quick tune to the resonance when the laser is turned on or drifts during operation.

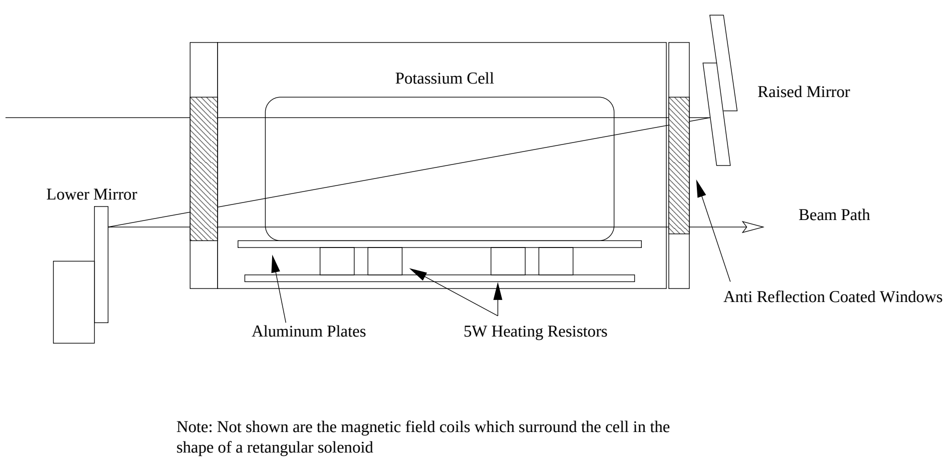

Figure 4: The housing and potassium cell from the side, showing the triple pass of the beams

4.2 Cell construction and difficulties

The cell itself is constructed by releasing a small amount of potassium into a vacuum (for the method, consult reference [7]). This means that there is a relatively low amount of free potassium in the cell equal to the vapour pressure of the potassium plated on to the cell walls. By heating the cell it is possible to free larger amounts of potassium by increasing the vapour pressure. To do this a plexi-glass housing similar to others used in the lab was constructed. The general layout of this can be found in Fig 4. This transition is about 30 times weaker than the transitions used to lock the other lasers [14] and so it is necessary to raise the cell to higher temperatures. In order to do this, two antireflection coated cell windows were purchased and installed on the housing and 4 power resistors were installed. Normally the cells in the lab use two 5W power resistors for heating. In this case the larger heating caused other problems, some of which took time to manifest themselves. The cell is supported underneath by a standard optics post and set screw through a threaded hole into the bottom of the cell. Currently the cell is run at approximately 18 W. By measuring the temperature as close to the bottom of the cell as possible we've found this corresponds to close to 100 degrees Celcius towards the resistors and drops rapidly towards the top of the box. We eventually found that this is sufficient to cause the plexiglass to soften at the bottom of the cell. Since the cell is not exactly symmetric about the post it began to lean to one side. When this was noticed it was alleviated by supporting that end of the cell and several metal bases were machined for future. Another problem is that there is a small amount of potassium in the cell, and a large temperature gradient. The windows of the cell are one of the cooler regions in the cell and as a result, considerable amounts of potassium began condensing on the cell windows. This would degrade the optical quality severely and make signals unusable. This problem was especially apparent when the cell was wrapped with the field coils, which served as an insulator for everywher on the cell except the cell windows. To fix this, it was decided to wrap the coils outside the entire box. The magnetic fields under this setup needed to be known at least approximately. A simple calculation was done using the Bio-savart law by taking the field at an arbitrary position for a square coil and numerically summing over all coils. For 2 A and 42 turns the field is approximately 8 G in the center of the cell and drops to 6 G towards the ends of the cell. To minimize this variation and increase the field the cell coils were wound out further along the box. In any position within the volume occupied by the cell the off-axis fields were found to stay at or below 0.5 G, and even then only when approaching the sides of the cell. This is the final configuration, except that 2 more sets of coils were wound around the original ones. To check these calculations, a gaussmeter was used to look at the field towards the end of the housing and just inside. The on-axis field was measured to be on the order of 6 G (with only the first set of coils on) which agrees fairly well with the calculated value. These fields are necessary for two purposes in the locking procedure. The magnetic field produces a Zeeman shift roughly equal to 1.4Mhz/Gauss. The current applied to the field coils is a sinusoid. This dither causes the transition frequency to oscillate assuming we circularly polarize the pump and probe beams, as opposed to the usual means of dithering the laser frequency [15].The dither allows the lock-in-amplifier (LIA) to pick up the signal. We would also like the dither to smear out the hyperfine structure so that the locking electronics is presented with a large capture region. This will be explained further in the locking section.

Further problems with this cell involving condensation of vapour on the inside of the housing windows. For all of these reasons it might seem better to try another cell design in future. It would be useful to distribute the heat more evenly in the cell to eliminate thermal gradients and support the base more firmly by using the metal bases obtained or an entirely non-plexiglass cell.

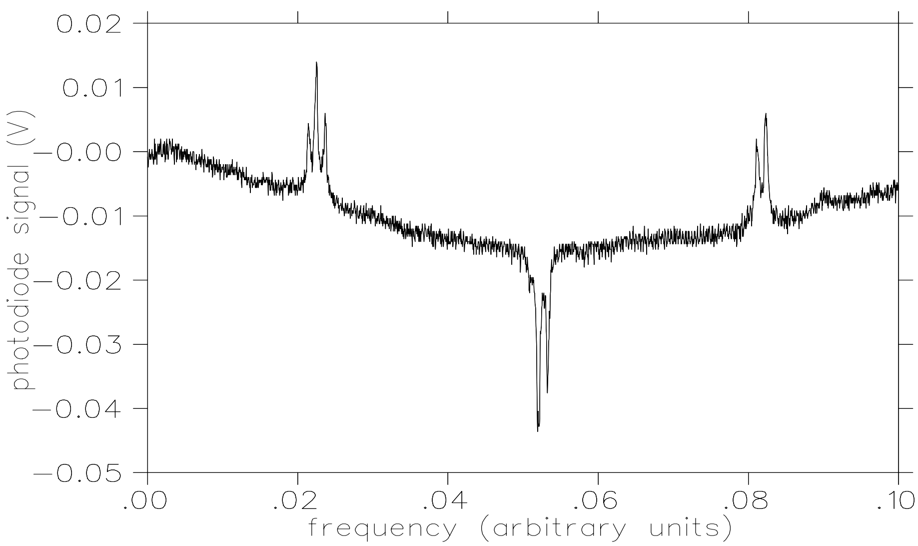

Figure 5: Saturation peaks on doppler broadened background for $4^2S_{1/2}$ to $5^2P_{1/2}$ transition

4.3 Saturation spectroscopy and signal detection

The saturation signal is detected by looking at a weak probe beam overlapping with a strong pump beam. In addition, there is another weak reference beam which is unsaturated. In order to obtain a true doppler free signal, the two are subtracted. For much of the initial work, the subtraction consisted solely of two photodiodes, oppositely oriented. A better subtraction circuit was later built using op-amps for current to voltage conversion, subtraction and gain. The schematic is included in the appendix. Three passes through the cell are used in order to enhance the saturation signal The problem unfortunately is that the optical quality of the cell windows is not perfect. This means that some positions in the cell will cause the beams to rapidly diverge or converge after the cell and also affects the beam quality since there are losses at each face and un-coated surface.

The saturation peaks could be observed on top of the doppler broadened background with some effort. The peaks observed are from ^{39}K because of the much greater natural abundance in the cell. The best signal obtained had saturation peaks of approximately 20% the height of the main doppler broadened background. A representative signal is shown in Fig 5. The entire doppler broadened background is not shown in this figure, but the curvature can be seen. Of the peaks shown, the macroscopic separation between the left and right set is due to the 461.7 Mhz ground state splitting stated previously. Two peaks in each correspond to the F=1 to F=1', F=1 to F=2' transition for the one ground state and F=2 to F=1' and F=2 to F=2' for the other. The third peak is the crossover peak. The oppositely going peaks are also crossover peaks, corresponding to the crossover dips discussed. In order to view the peaks in finer detail the scan voltage is decreased and the offset can be used to focus on individual sets of peaks. As they have the clearest structure, this was performed on the furthest left set of peaks. These correspond to transitions from the F=2 ground state. By narrowing in on this set of peaks, and then recording it we could get an estimate of the current linewidth, with no locking mechanism. To do this the signal shown in Fig 6 was fit to three summed Lorentzians with a linear sloping background to take into account the doppler broadened background. The closest fit obtained gave the the numbers found in Table 4.3.The centroids positions were converted to frequency by using the known 18 Mhz separation, and frequencies listed relative to the leftmost peak. The halfwidth value was

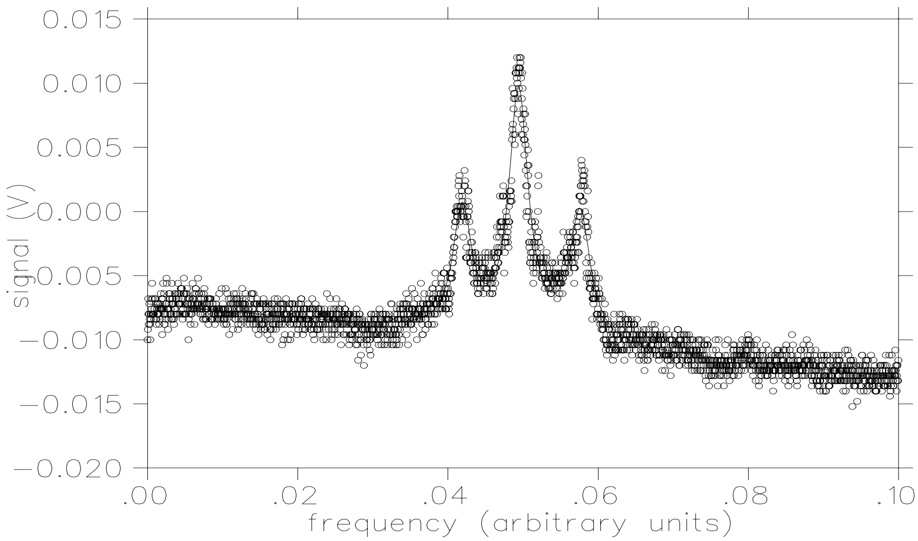

Figure 6: Fit of 3 saturation spectroscopy peaks

similarly converted.

peak	centroid(Mhz)
1	0
crossover	8.59
2	9.39
half-width (Mhz): 1.82	

Table 1: A simple three-Lorentzian fit to one set of ^{39}K saturation peaks

There is only one halfwidth listed here as several fits were run and this particular run utilized only the one sigma for all three peaks. This is not absolutely correct given that some effects such as power broadening can depend on the strength of the transition and the crossover peak may have different behaviour, but this fit gives a comparable number to fits done using three separate σs . For real accuracy the peaks should be fit using Voigt profiles but this would have to be done numerically. As the two furthest separated peaks are 18 Mhz apart we can find that the FWHM is approximately 3.7 Mhz. It could actually be slightly better or worse than this as the fitted curve does not reach the maxima of the peaks and the poorer diode and subtraction setup used introduced more noise. The purpose of the fit is more to demonstrate the structure of the saturation signal and estimate the peak widths more accurately than by eye.

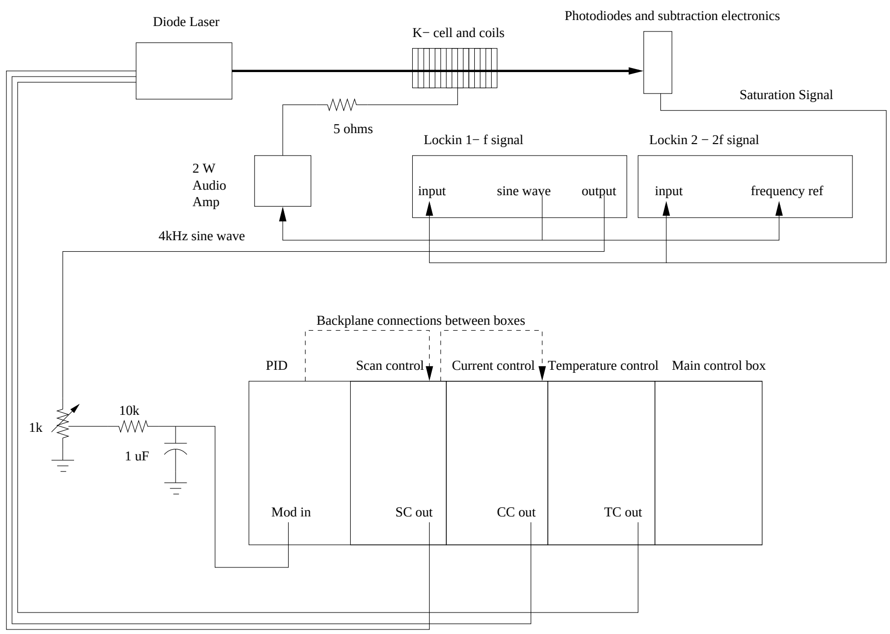

Figure 7: Schematic diagram of the electronics setup for controlling the laser

The saturation spectroscopy produces a signal as shown above. A LIA is used here to create a zero crossing signal. For the general arrangement refer to Fig 7. The first LIA has a dual purpose, it generates the sine wave used to dither the cell and produces a zero crossing low noise signal from which to create the lock. The dither on the cell, as explained earlier, smears out the peak structure observed on the LIA signal. This, in combination with integration on the LIA, creates a relatively flat slope which is ideal for locking. The 4 kHz dither rate was chosen by observation. The saturation signal was fed to the LIA, and by adjusting the height of the dithered signal, the lockin phase, and the frequency it was found that the saturation peaks could be smeared out. The structure at this point is shown in Fig 8. Note that the structure is not yet fully smeared out. This is prior to adding the

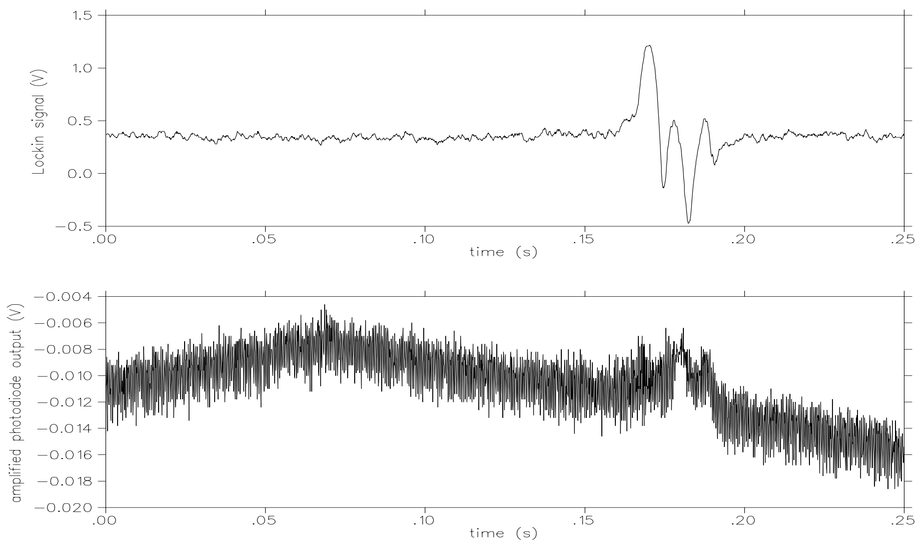

Figure 8: Peaks for transitions from the F=2 state

second and third set of coils and the integration box on the modulation input of the PID controller shown on Fig 7.

Further, note that the amplitude of the LIA signal is on the order of 1V. If we were to add this back into the modulation input of the PID it would be very difficult to lock. In the simplest sense, locking the laser requires a zero crossing signal on a particular frequency which adds a voltage correction whenever the laser moves away from that point. It was found that the separation between the $5^2P_{1/2}$ peaks was approximately 50 mV on the scan control. Alternatively, it was found that the 460 Mhz separation between the ground state peaks was on the order of 1.4 V. This allows us to understand frequency scale on the scan control to be approximately 55(5) mV for 18 Mhz, or 0.00303(31) Mhz/V. This means that applying a 200 mV signal initially would change the frequency on the order of 80 Mhz from the desired position. This would mean that the laser would be outside of the actual voltage region in which the peaks lie, and the locking signal would vanish. In order to compensate for this a temporary solution was to insert the 1K variable resistor shown in the diagram in order to reduce the signal amplitude. This unfortunately does introduce some noise on the signal. What might be preferable is to use a more stable electronic circuit to reduce the signal amplitude.

What is also visible here is that the addition of the dither has largely overwhelmed the saturation peaks directly from the diode circuit. At this point this signal is of less use than the LIA signal. In order to monitor the actual position of the signal and try to get a sense of how effective the lock is a second LIA is used. This LIA takes the second derivative of the input signal, but is not smeared out by extra integration and deliberate misadjustment of the phase. Thus once the laser is locked it is possible to watch this "2f" signal and observe whether it rests on a single peak or jumps across several. This gives an estimate of the how narrow a range the frequency of the laser is being maintained over. This signal is shown in Fig 9.

The PID control box included with the laser has some complications and is currently not working correctly. This is why the second LIA is included as a diagnostic. In the interim, the signal from the first LIA is sent across the 1k potentiometer and through a 10 ms integrator to smooth out fast noise. In then enters the modulation input of the PID box. This input is designed to allow the user to add a modulation signal on top of the PID output directly to the scan output to the laser. This is the high voltage model which means that the mod input is scaled by 15 times, in order to take a -10 - +10 V input into 0-150 V. If there is any portion of the scan control voltage which then falls below zero it is ignored by the piezo stack which will not accept negative voltages. This method of adding the voltage is used because the original scan control voltage was on the order of 140 as mentioned previously. This would have meant adding a several mV signal accurately to a 140 V offset. This seemed to be the only stable means of doing so currently.

With this locking setup, in theory we should simply be able to throw the ramp switch on the PID and thus add the signal to the scan control while turning the scan range down. Then if the signal is away from zero, or the laser drifts away from zero, a voltage in the opposite direction would be applied to correct. When this was attemped it seemed at first that the laser was locking correctly and resting either at the top of a 2f peak or moving alongside a single peak. The complicating factor is that whatever is observed on the LIA signal before the mod input is then multiplied by 15 times. This we think has the unfortunate effect of multiplying any noise as well. This is not a large problem with the signal as a whole, but when locked the signal need be free of noise to several mV in order to maintain the frequency to 1 Mhz. Another measure of how well the lock is behaving is the vertical size of the f signal. Since the f signal is being fed directly back

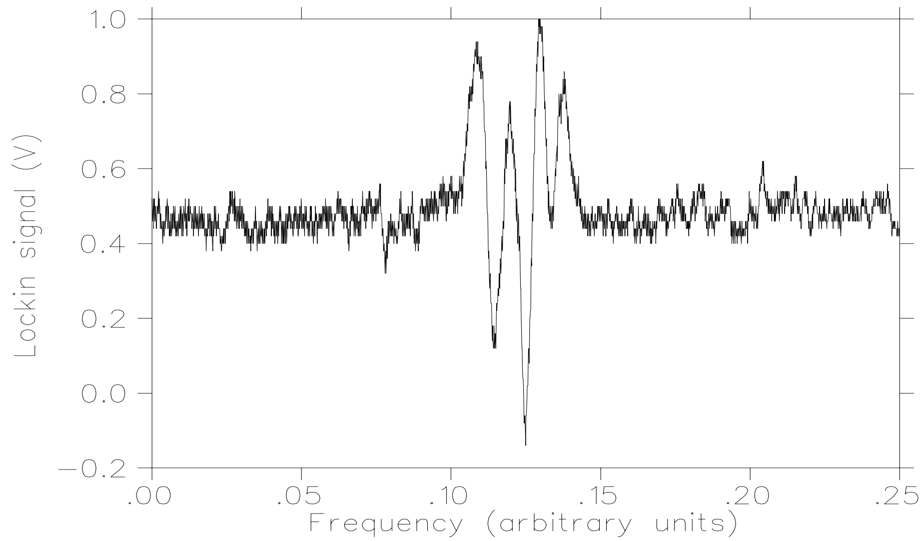

Figure 9: 2f signal obtained on the F=2 to 1 and F=2 to 2 transitions

into the mod in (and through the multiplication) the vertical jitter on the signal should roughly correspond to the locking jitter. This unfortunately varies considerably based on the settings for a particular run. A typical size observed is 5(1) mV vertically. If this is strictly from the laser signal then we could infer that this is on the order of 5/55 or about 1.6 Mhz. However, because the signal is passing through the multiplication this may then mean that it is closer to a 20 Mhz noise on the signal. This is not well understood.

After some further attempts to use the PID controller it was found that "locking" no longer appeared to remain on a single "2f" peak. By turning down the 1k pot, or changing the sensitivity it seemed the lock could be improved at the expense of the capture range and possibly longterm stability. While in this state, the laser did appear to compensate for accoustic noise and so seems nominally locked, though not to the necessary 1 Mhz. The most effective way to test this of course will be to use the laser to attempt to probe the polarization. This is discussed below. First however, keeping in mind the tenous nature of the lock, which seems only stable for minutes at most, the AOM shift of the laser frequency should first be discussed.

4.4 Frequency shift using a 300 Mhz AOM

Refer back to Fig 3 for the alignment of the AOM setup. The beam is picked off by changing the laser polarization from linear vertical to circular using a $\lambda/4$ and then sending the vertical component of the beam through to the trap line and allowing the horizontal to pass through a polarizing beamsplitting cube. This is then rotated back to vertical by means of a $\lambda/2$ and sent to the saturation spectroscopy setup. The beam to the AOM path is reflected at a right angle using another cube and then through the AOM from there. The mechanics of AOM function will not be discussed here, but crudely speaking the sound field induced in the crystal acts much as a diffraction grating and creates several orders of the beam at multiples of the Bragg angle. The deflected orders are frequency shifted up or down by the frequency of the RF driver used. For this transition, since the isotope shift from 39 to 41 is on the order of 450-500 Mhz it is not possible to shift using a single typical AOM which can do less than 200 Mhz single pass. For the purposes of this beam a 300 Mhz AOM is used from Intraaction. The coatings on the face of the crystal are however optimized for IR wavelengths, so even before the AOM there are significant reflection losses in the beam. Following the AOM there are essentially two orders observed , the deflected first order and the unaffected though weaker power zero order beam. Both are sent through another $\lambda/4$ and a lens to make the 2 parallel along part of the path. The quarter wave plate changes the polarization to circular on the first pass, and then rotates again to horizontal on the return path. An iris is used to eliminate the zero order beam. The first order beam returns through the AOM and creates two orders of its own which pass through the cube (note the different polarization) and onto the trap. The beams which return through the AOM are singly and doubly diffracted versions of the original laser frequency. The doubly diffracted beam, which is shifted by twice the RF frequency is sent through a telescope to expand it from 1-2 mm to just under a 1 cm diameter. This is then sent to the MOT. All of this beam path is independent of the locking setup and is reasonably well set up. The power measured along this path is approximately 85 μW going to the trap. This seems like relatively little power, however consider that aside from reflections the AOM has approximately 65 % efficiency on the first pass included reflection losses and 42% on the second. Part of the reason for this is that the material used in the AOM , TeO_2 is less efficient for one polarization than the other.

4.5 Specific Mass Shift Measurement and Polarization tests

The isotope shift was estimated previously using the calculated NMS in addition to the SMS and FS for the ground to $4^2P_{1/2}$ state. This was found to be 475.77 Mhz. In order to excite atoms in the ^{41}K F=2-1 and F=2-2 states it is necessary to know the total isotope shift well. There are two ways available to do this given the current apparatus.

If the laser is locked, the RF frequency to the AOM can then be scanned over the theoretical range in which the states should lie. This however assumes that the isotope shift is sufficiently close to the initial estimate that the scan encompasses. The scan is performed using a DAC with a finite number of steps which limits the range over which the AOM is scanned as a larger range involves larger DAC steps and thus larger steps. Should the steps be larger than 1 Mhz it is possible the resonant states could be missed entirely. Scans were performed of up to 20 Mhz, with 0.6 Mhz steps. Frequency ranges between 508 and 556 Mhz were attempted in segments. To observe the signal, other lasers at 355 nm, and 532 nm were also used which should be capable of photoionizing these states to the continuum. To detect the signal the ions would then be detected using the microchannel plate in the trap by requiring the appropriate cooincidences. No signal was observed however. Attempting to use the 769.9 nm light from the other diode laser to increase the signal was also attempted however this yielded no larger signal.

Alternatively we can use the saturation spectroscopy signal itself to estimate the isotope shift and from this the residual isotope shift. This encompasses the field shift as well as the specific mass shift but excludes the normal mass shift which is easily calculable. Performing this measurement assumes that both the ^{41}K and ^{39}K signals can be viewed on the scope simultaneously. This is shown in Fig 10. Note that the signal size for ^{41}K is considerably smaller, being just detectable. On these signals the substructure has been smeared out and it is believed that the leftmost peak shown is the F=2 to 1 and F=2 to 2 transitions together with the crossover peak. Thus the main zero crossing is thought to be the crossover peak center which is -2.25 Mhz

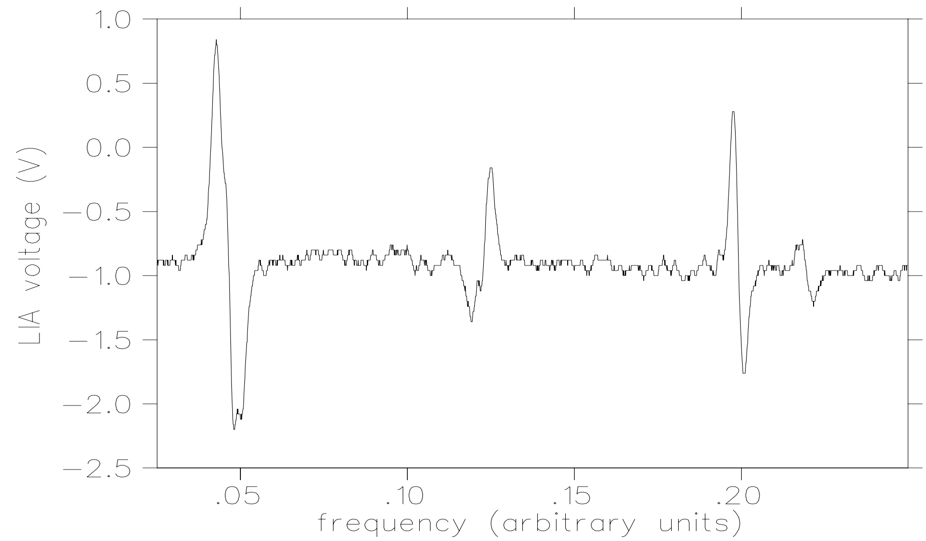

Figure 10: Lockin peaks for ^{39}K and left most or F=2 ^{41}K peak

relative to the center. The peak on the right however is thought to cross at the F=1 to F=2 transition. This is because the F=1 to F=1 transition has roughly 1/10th the strength of the other based on known transition rates [16] and we don't observe it even with the best saturation signal. Thus the separation between these two points is $461.719 + 6.74 + 2.25$ Mhz, or 470.71 Mhz. Based on three separate plots which were in agreement to within 2 Mhz, the frequency separation from the ^{39}K F=2 crossover to the ^{41}K peak was found to be 535(5) Mhz. The uncertainty on this is primarily due to the fact that the ^{41}K structure is completely unresolved and so the location of the zero crossing signal is uncertain to at least that degree. We can then use this to calculate the isotope shift and compare to our theoretical value. We can assumed that to this degree of accuracy the hyperfine splittings are exact and so the isotope shift is $533(5) - 173.54 - 2.25 + 95.26 = 454(5)$ Mhz. This is considerably different than the 476 Mhz calculated earlier. If we assume the field shift remains relatively constant as discussed previously than this would require the SMS to be some 22 Mhz larger for this transition.

As a check, the transition was also measured using a slightly different method. The dither power to the field coils was reduced from around 2.94 VAC to 2 and the phase and time constant on the lockin changed to try and better resolve the peak structure. A scan of the F=1 peaks and the

^{41}K peaks were then taken and compared. Only two peaks were observed as usual, but the peak structure was better resolved. This is shown in Fig 11. Again, it is assumed the peak structure is made up of the F=1 to 2

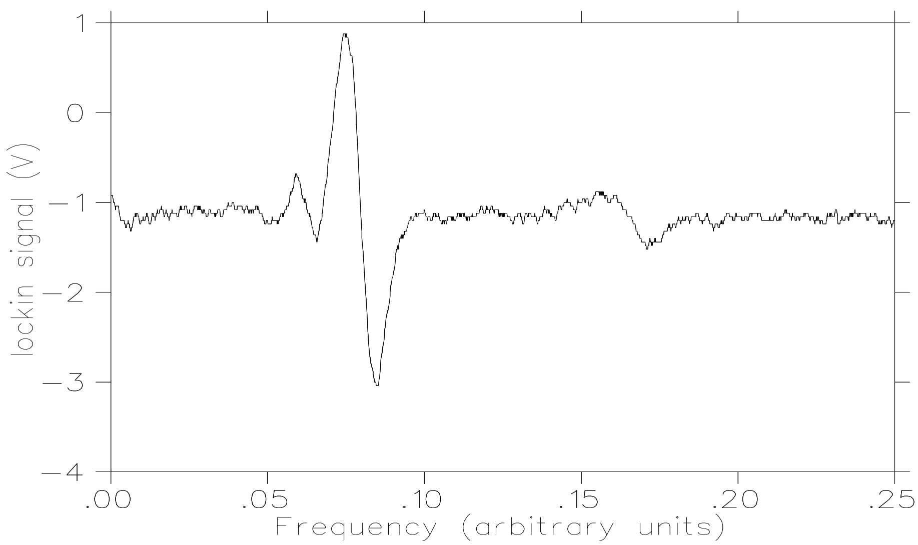

Figure 11: Better resolved F=1 peaks with 41 F=2 peaks

transition and the crossover peaks. Similar to the previous calculation this gives a separation from the F=2 ^{39}K crossover to the ^{41}K F=2 crossover of 514(5) Mhz. From this an isotope shift of 433(5) Mhz. This is surprisingly smaller than the previous result. A residual isotope shift which is 21 Mhz larger would be required to account for this change. Only a single scan was taken of this number, but the peaks are better resolved. It is possible that this was a poor scan or some other effect. Given more time it would have been advantageous attempt this scan again and try to fit all the main peak structures on the scan. This frequency only just lies within the scan range looked at in the tests so it is possible that this is the reason there was no sizeable signal.

All of these measurements assumed excellent linearity PZT. This was cross-checked using the middle zero crossing signals generated by the ground state crossover peaks. In each measurement the separation between the ground state and the crossover peaks was looked at and all pairs of measurements agreed to within 2.5 % with no obvious trend over the 460 Mhz.

5 Conclusions

The laser is now set up in what is hopefully the final configuration. Depending on the tuning of the AOM sound field to the laser beam approximately 93 μW are delivered to the trap. This power might be improved by further tuning of the laser frequency but is reasonable given the losses observed throughout the path and the AOM efficiencies.

The saturation spectroscopy setup is now in place though some minor adjustments to the cell to ensure the potassium does not pool at the coolest part of the cell would be helpful. These adjustments could be as simple as adding some form of heating element to the bottom of the cell to force the neck of the glass cell to a higher temperature.

The hyperfine structure of both ^{39}K and ^{41}K were calculated in order to understand the saturation signal better. These are listed in section 2.

By looking at the saturation signal we can conclude that the linewidth is less than or equal to 3.7 Mhz. The saturation signal shows a well defined zero crossing signal that is reproducible. In order to lock it would be better if the PID box were functioning, but even without it is thought that the laser can be locked. The actual width of the lock can't be easily measured until we are capable of scanning across the resonant lines and finding the signal using the photoionization signal from the trapped atoms. This has not been successfully demonstrated yet. The lock observed currently persists for only several minutes in general. This is a result of the laser frequency drifting up to 60-80 Mhz over this time period which then exceeds the capture range of the lock.

Using the saturation signal a temporary measurement of the isotope shift was obtained. The isotope shift obtained was 454(5) Mhz. Another measurement using only the ^{39}K F=1 to 2 and F=1 crossover peaks was also attempted resulting in a shift of 433(5) Mhz. The two measurements are not in agreement, however the second method was only attempted once, and should be repeated if the shift is to be better understood. This may not be necessary since the shift can be much better understood if the nuclear signal is observed which would give the frequencies to Mhz accuracy.

The SMS shift given by either method for the $5^2P_{1/2}$ state is much larger than the literature value for the $4^2P_{1/2}$ state. This is an interesting atomic physics result if it can be better quantified.

6 Acknowledgments

I had another excellent experience here at TRIUMF this summer and want to thank the people with whom I worked and played.

John Behr and Matt Pearson were invaluable with their help on the laser. I don't know if I would have gotten anywhere without John, though I think perhaps now I would know enough to begin to do so. I started from scratch on the atomic and nuclear aspects of this spectroscopy and learned a lot with their help as well.

Other members of the group such as Sihong Gu, Dan Melconian, and Peter Jackson were very helpful and supportive, especially in understanding the arcane systems that nova and physica comprise.

Frank Berghaus, Mike Lamey, as well as our volleyball team A (which came so much closer than last year!) were great fun.

It was an excellent experience, I hope I come back to TRIUMF someday in some capacity.

A Appendix: Circuit Diagrams

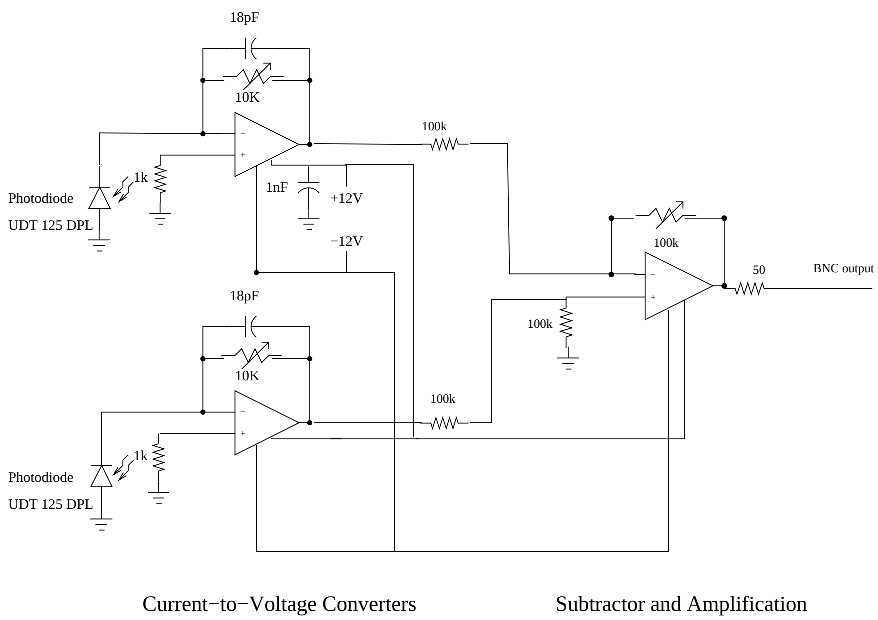

Figure 12: Diode Subtraction Circuit and Amplifier

References

[1] Chu, S., Reviews of Modern Physics, 1998, **70**, 685.

[2] Vollrath, I., 2001, Summer Workterm Report (untitled).

[3] NIST Atomic Spectra Database Levels Data http://www.physics.nist.gov/PhysRefData/contents-atomic.html accessed Aug 2002.

[4] Demtroder, W., Laser Spectroscopy, Berlin:Springer Publishing, 1996, 437.

[5] Pearson, M., Chapter 2 - PhD Thesis, 1998, Unversity of Manchester, unpublished.

[6] Arimondo, E., Ingusico, M., Violino, P., Reviews of Modern Physics, 1977, **49**, No. 1, 31.

[7] Eaton, S., 2000, Saturation Spectroscopy of Potassium, Summer Work-term Report.

[8] Raghavan, P., Atomic and Nuclear Data Tables, 1989, **42**, 189.

[9] King, W. H., Isotope shifts in atomic spectra, New York: Plenum Press, 1984, 16.

[10] University of Manchester Nuclear physics group http://nuclear.ph.man.ac.uk/~rm/node6.html, accessed Aug 2002.

[11] Martensson, A., Salomonson, S., J. Phys. B:Atomic and Molecular Physics, 1982, **15**, 2115.

[12] Martensson-Pendrill, A., Pendrill, L., Salomonson, S., Warston, H., Ynnerman, A., J. Phys. B:Atomic and Molecular Physics, 1990, **23**, 1749.

[13] Wendt, K., Ahmad, S., Buchinger, F., Mueller, A., Neugart, R., Otten, E., Z. Phys. A, 1984, **318**, 125.

[14] Personal communication: John Behr

[15] Chung, Y. C., SPIE , 1992, **1837**, 70.

[16] Metcalf, H., van der Straten, P., Laser Cooling and Trapping, New York:Spring Publishing, 1999, 284.

[17] Personal communication: Matthew Pearson